European Journal of Mechanics B/Fluids 59 (2016) 161–168

Contents lists available at ScienceDirect

European Journal of Mechanics B/Fluids

journal homepage: www.elsevier.com/locate/ejmflu

Experimental and numerical studies of low aspect ratio wing at critical Reynolds number

Po-Wei Chen, Chi-Jeng Bai, Wei-Cheng Wang *

Department of Aeronautics and Astronautics, National Cheng Kung University, Tainan, 70101, Taiwan

ARTICLE INFO

Article history:
Received 5 September 2015
Received in revised form
18 March 2016
Accepted 10 June 2016
Available online 16 June 2016

Keywords:
Laminar separation bubble
Low-aspect-ratio wing
Critical Reynolds number
Computational fluid dynamics
Wind tunnel experiment

ABSTRACT

In this study, the three-dimensional flow behaviors and aerodynamics characteristics of a NACA0003 wing with an aspect ratio (AR) of 1 at Reynolds numbers of 1.0×10^5 has been investigated both experimentally and numerically. The force measurement and flow visualization (oil flow visualization) through the wind tunnel experiment were applied to verify the reliability of the simulation. The investigation with different angles of attack reveals that flow structure contained three dimensional laminar separation bubble (LSB) and wing-tip vortex. As increasing angle of attack, the area occupied by LSB expands both streamwise and spanwise. The wing-tip vortex has strong impact on the formation of LSB. In addition, the spanwise load distribution has shown that both three dimensional LSB and wing-tip vortex provide additional vortex force.

1. Introduction

A large number of applications associated with low aspect ratio (LAR) wing at critical Reynolds numbers have been developed rapidly such as micro air vehicles (MAVs), unmanned aerial vehicles (UAVs). UAVs and MAVs operate at low chord Reynolds numbers (Re_c) ranging from 10^4 to 10^5. This range of Re containing the transition from laminar to turbulent flow is so called critical Reynolds number region. In general, the laminar separation bubbles (LSBs) found on the leeward surface of the wing at critical Reynolds numbers have significant impacts on aerodynamic performance especially for the two-dimensional (2-D) cases [1,2]. The sensitive boundary layer at critical Reynolds numbers leads to the difficulties in understanding the phenomenon of LSB. Currently studies have been conducted on locating LSBs on 2-D wing section with end plate [3]. The formation of LSB is affected by the Reynolds number, angle of attack, pressure gradient, free stream turbulence and surface roughness. Meara and Mueller [4] revealed that the LSB decreases in length and thickness as Reynolds number is increased, and a linear relationship exists between those of the separation bubble.

The flow structure surrounding three-dimensional (3-D) LAR wing is typically complex including three-dimensional wing-tip vortex, separation, reattachment, and transition. With the complexity of the flow structure, the performance of LAR wings at critical Reynolds numbers is influenced by many factors. The most important factor is aspect ratio (AR), following by the wing planform and Reynolds numbers. In addition, as AR is less than 1.25, relatively high maximum lift coefficient occurs for the rectangular planform wings [5]. The higher maximum lift curve results from the vortex system around the wing. This vortex system provides not only extra lift but also drag.

Visualizing the flow field structure helps understand the aerodynamics of LAR wings at critical Reynolds numbers. Many flow visualization techniques have been applied, including oil flow visualization, high-resolution particle image velocimetry (PIV), and thermographic method to picture the formation of LSBs for 2-D cases [6–8]. For 3-D cases, numerical approaches have been used with appropriate transition models. Wilcox [9] accurately described several transitional boundary layers and nonlinear growth of flow instability using the k–ω two-equation turbulence model. Chen et al. [10] predicted the formation and suppression of LSBs caused by 3-D effects on a cambered thin wing with the AR of 6 at low Reynolds numbers using the k–ω shear-stress transport model. Experimentally, Bastedo and Mueller [11] determined the location of LSB through measuring the pressure distribution of Wortmann FX 63-137 wings with AR of 2. At lower Reynolds numbers such as $Re_c = 8.0 \times 10^4$, wing-tip vortex induces large spanwise flow component which results in the spanwise variation of 3-D LSBs. However, neither experimental nor numerical observations on flow structure of LAR wings (aspect ratio less than 2) at critical Reynolds numbers is clear.

* Correspondence to: 1 University Rd., East District, Tainan, Taiwan.
E-mail addresses: wishfly227@gmail.com (P.-W. Chen), chijeng.bai@gmail.com (C.-J. Bai), wilsonwang@mail.ncku.edu.tw (W.-C. Wang).

http://dx.doi.org/10.1016/j.euromechflu.2016.06.005
0997-7546/

The primary objective of the present research is to understand the 3-D flow structures including the interaction between tip vortex and LSBs and the aerodynamic loading of LAR wings at critical Reynolds numbers. The experimental and numerical flow visualizations were carried out with the NACA0003 wing with AR of 1 at Reynolds number of 1.0×10^5.

2. Experimental

The force measurements and the flow visualizations were carried out in an open-type and subsonic low-speed wind tunnel located in the Department of Aeronautics and Astronautics at the National Cheng Kung University, Tainan, Taiwan. The nozzle contraction ratio is 9 to 1 and the dimension of the test section is 1440 mm $\times$ 1200 mm $\times$ 914 mm. The freestream velocity, U_∞, near the center of the test section can be operated from 5 to 35 m/s. In this study, the experiments were conducted at Re_c of 1.0×10^5. The desired wind speeds can be reached within 15 s. The turbulence intensity of the wind speed for present study is approximately 0.165%. The testing wing is the rectangular NACA0003 airfoil with the chord length (c) of 15 cm and AR of 1. For the purpose of visualizing the flow, the black Acrylonitrile Butadiene Styrene (ABS) was chosen as the material, which paints the black matte over the surface.

2.1. Force measurement

The six-component external strain gauge (WM-19-2B, JEOOU RONG Industrial CO., LTD., Kaohsiung, Taiwan) was installed at the bottom of the wind tunnel to measure force and moment acting on the wing as shown in Fig. 1. The loading constrains are 5 kg in z-axis, and 3 kg in both x-axis and y-axis. After calibration, the accuracy of each force measurement can be reached to $\pm$ 2 g. The aerodynamic coefficients were obtained by averaging 30 000 samples acquired at a frequency of 1000 Hz. In order to control the α of the wing, the wing and force balances were connected with the angle of attack control system, consisting of a wing support with a digital servo (Futaba S9156). The front cylinder was fixed and supported along the quarter chord axis of wing model. The back cylinder which connected with the digital servo was used to control the angle of attack of the wing model by pulling downward and pushing upward of the tail of the wing. After the setting of the angle of attack was achieved by the digital servo, the position of servo was fixed to ensure the validation of the experiment. The model was installed at the center of wind tunnel and the area blocked by the model and the supporting device for all the cases is less than 1% of the sectional area of the test section. In this study, with low speed condition, the wall effects are neglected.

2.2. Oil flow visualization

Oil flow visualization was additionally applied to observe the flow pattern on the leeward surface of the testing wing. The positions of laminar flow separation, oil accumulation and reattachment were observed. Researches indicated that, through the leftover oil pattern, the formation of laminar flow, T/S waves, spanwise vorticity, 3D vortex breakdown, turbulent spots and fully turbulent flow can be clearly observed [7]. The inertia forces of the oil mixture should be lower than the viscous ones to avoid the influence of the surface condition. The oil mixture is composed of Titanium Dioxide (TiO_2) (Santoku Chemical Company, Osaka, Japan), kerosene (113F 4100069, CPC corporation, Taiwan) and oleic acid ($C_{18}H_{34}O_2$) (DC-O01, Honli Chemical Company, Chiayi, Taiwan) with mass ratio of 6:12:1. Before the test, the model was coated with oil mixture. As the air flowed over the surface, the steaks marked by the oil represented the skin friction lines (limiting streamlines) over the wing surface.

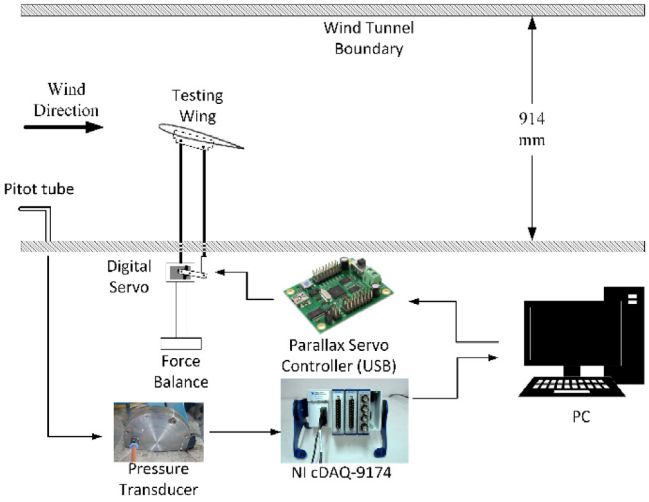

Fig. 1. Setup of the wind tunnel experiment.

3. Computational method

3.1. Methodology

ANSYS Fluent^{TM} version 14.5 was used for the simulation, with The SIMPLE algorithm and a second-order upwind scheme to solve the steady-state Navier–Stokes equation. To have better prediction of the flow field near the surface of the model and the transition flow, the SST k–ω model, transition SST model, and K–kl model were selected as the turbulence models. The results showed that transition SST model and K–kl model failed to predict the laminar separation bubble above the wing. Based on two-dimensional simulation, the SST k–ω model was selected as the turbulence model. The vortex systems were addressed by comparing with experimental results. Each computation consists of 5000 iterations. Convergence with residual level of 10^{-3} is normally reached after approximately 1500 computations.

3.2. Grid and boundary condition

Three dimensional grids were generated for NACA0003 airfoil with chord length of 1 and aspect ratio of 1. The origin of coordinate was set at the mid-section of the leading edge. To verify the accuracy for predicting lift and drag profiles of the airfoil, a series of two-dimensional tests with various turbulence models were carried out and compared with wind tunnel experiments.

The meshing software Pointwise (version 17.0) was used to generate the grid system. The domain of the NACA0003 wing is a cuboid. The upstream is 5 times of chord length from the leading edge towards front and the edge of pressure outlet is 10 times of chord length from leading edge towards aft. The periodic boundary of the computational domain was expended to 5 times of the chord length at upper and lower side of the wing and to 2.5 times of the span length at left and right side of the wing. Inside the computational domain, the mesh is a hybrid mesh composed of structure and unstructured grids. In order to simulate the detail flow field on the surface of the wing, thirty layers of structure grid with grow rate of 1.1 were generated around the airfoil to calculate the boundary layer flow as shown in Fig. 2. In this study, simulations were carried out with the same conditions as wind tunnel tests, which is close to the free flow condition. Conditions for the boundary are pressure, 101,325 pa; Reynolds number, 100,000; temperature, 300 K; and turbulence intensity, 0.165%. The direction of the flow is specified in Cartesian coordinates and depends on the angle of attack. The Reynolds number chosen as